Impact of an Applied Magnetic Field on a High Impedance Dual Anode LANR Device

Mitchell R. Swartz*

This paper was presented at the March 2010 New Energy Technology Symposium, a session at the 239th American Chemical Society national meeting. It also appeared in the Journal of Condensded Matter Nuclear Science (Issue 4, pp. 93-105, 2011).

Abstract — *This paper reports on the impact of an applied magnetic field intensity on LANR solution electrical resistivity and an analysis of the impact on LANR performance through loading. A dual anode PHUSOR®-type Pd/D_2O/Au LANR device was driven at its optimal operating point, with two electrical current sources, to drive, and examine by 4-terminal electrical resistance, the loaded PdD_x cathode. An applied magnetic field ~0.3 T increases the LANR solution's electrical resistance ~10-17% with a time constant in minutes. The incremental resistance increase to an applied H-field is greatest at low loading current. The incremental resistance increase from an applied H-field is greatest with the applied H-field perpendicular to the driving electrical field (E-field) intensity. The modified LANR deuteron loading rate equation indicates that an applied magnetic field intensity increases deuteron loading in an LANR system by the increasing solution resistance.*

1. Lattice Assisted Nuclear Reactions

Lattice assisted nuclear reactions (LANR) use hydrogen-loaded alloys to enable near room temperature deuterium fusion and other nuclear reactions[1-49] using deuterons as fuel. Technologies which increase LANR excess energy production include thermal power spectroscopy,[4] optimal operating point operation,[1,3,4,24] the use of high electrical impedance solutions,[3,4] metamaterial shapes[1,32] and nanostructures.[1,37,60] Correctly driven, LANR metamaterial nanostructured devices exhibit excess heat, excess heat flow and non-thermal near infrared (NT-NIR) emission linked to both.[34] LANRs generated ("excess") power densities range from ~7 (1989 announcement) to 80-10,000 W/cm^3, today. Over time, the magnitude of generated excess power yields significant excess heat and material changes which are wrought on the electrode, such as volcano-like pits.[8,18,19]

At LANRs "core" are deuterons which are tightly packed into binary ("highly loaded") metals and metallic nanostructures by an applied electric field or elevated gas pressure which supply deuterons in heavy water or gaseous deuterium. With control of LANR devices by precise nanostructure fabrication, metamaterial shape selection using high impedance ("High-Z") PHUSOR®-type LANR devices in very high electrical resistivity (the real part of the complex impedance, with units of ohms) D_2O, control of D-flux and post D-loading flux, there is a higher likelihood of achieving LANRs impressive energy gain, and with time integration—excess heat, and with fairly good reproducibility.

Dual anode PHUSOR® (DAP) LANR devices use two anodes. The first is for preparation of the codepositional surface and solution, and the second is used to drive the active surface.[37,68] Investigations of DAP LANR devices (Figure 1) have demonstrated that nanostructures are important in LANR with sizes involving circa 10 atoms or more in size. Corroboration of this fact includes experimental results in codeposition[25] and NT-NIR (Figure 3) emissions.[34] The curve in Figure 1 demonstrates with experimental evidence that LANR excess heat is correlated with the size of the Pd–D nanostructures, which can be considerable (Figure 2). Figure 1 shows the monotonic increase in excess heat from LANR as the codepositional layer was increased in size over loaded palladium, apparently beginning with nanosize structures in temperature (degrees centigrade, delta-T) for both the ohmic thermal control and the DAP-type LANR device. The input power normalized delta-T was used to compare the LANR and control (ohmic) systems over varying input powers. Sites 1 and 2 represent two sites within the active LANR cell. Site 3 was located at the ohmic (joule) control, consisting of a carbon resistor. In Figure 2, over time, electrical power was first delivered to the control and then to the LANR device. The important point is that Figure 2 demonstrates an LANR power gain of ~8000%.

By imaging near infrared (NIR), Figure 3 shows a distribution of LANR activity over the surface of an LANR device, consistent with nanostructures. It shows the emission of near-IR from the electrodes when excess heat is only observed and the active electrodes operated at their optimal operating point (OOP[1,2,57]), and then the NT-NIR emission is linked and specific to the LANR devices' excess heat production and not its physical temperature.[34] This results from the temperature-related shift from hot fusion's penetrating ionizing radiation to LANR's skindepth-locked infrared radiation.[50] Unlike hot fusion or plasma systems, Bremsstrahlung radiant power density falls from 0.05 to 0.28 (hot fusion) to 1.4-8.1 x 10^{-10} for LANR. The delivered X-ray dose at 1m decreases by

incredible 18-23 orders of magnitude from 3.1 x 10^{19} Grays (hot fusion) to ~2 x 10^{-4} Grays for LANR. In addition, the temperature difference also causes the output spectrum of the Bremsstrahlung radiation to be shifted to the NIR, consistent with the NIR emission of LANR systems at their OOP. Figure 3 shows three visible and NIR views of a DAP codeposition PHUSOR®-type LANR device in heavy water. The platinum anode is seen in the background. The DAP is located in both images (~7.7 mM $Pd(OD)_2$). The inset view is in ordinary light, the other two (from a slightly different angle of observation) are in the NIR. The image on the left precedes ("off"), and the one on the right is after activation and generation of excess heat of the PHUSOR®-type LANR system.

Given these LANR reactions, there has been much interest in the application of magnetic field intensities to LANR systems. Dr. Pamela Mosier-Boss *et al.* at SPAWAR have reported morphology changes on the cathode with an applied magnetic field intensity.[19] For reasons that will become clear in the Interpretation section, because of the complex impact of laser irradiation of LANR cathodes upon solution electrical resistance and power gain,[33] we elected to first report on the effect of those applied magnetic field intensities on LANR solution's electrical conductivity because that material parameter is decisive in the success of LANR systems.

2. Experimental Details

The six terminal LANR codepositional high impedance device used here was a DAP LANR device (Pd/D_2O, $Pd(OD)_2$/Pt–Au). It contains nanostructures whose preparation, assembly and driving is complicated and described elsewhere.[1-4,34,35,37] The LANR cathodes were prepared from 99.98+% Pd [Alfa Aesar, Ward Hill, MA], 1.0 mm diameter, ~4-7 turns on a spiral of ~1.3 cm diameter, with a gap separation from the anode arranged in a Pd/D_2O/Pt or Pd/D_2O/Au configuration (Pt 99.998%). The solution was 7.7 mM $Pd(OD)_2$ in low paramagnetic high electrical resistivity heavy water (deuterium oxide, low paramagnetic, 99.99%, Cambridge Isotope Laboratories, Andover MA) with no additional electrolyte. For the DAP devices, palladium is laid down from a sacrificial anode upon the surface of a palladium cathode. Then, the palladium anode is removed and replaced by a gold wire anode to stop the further laying down of palladium nanostructure upon the palladium cathode. Interestingly, we have reported a new phenomenon during codepositional layering of the DAP cathode. This consists of a dynamic instability oscillation, an electrohydrodynamic Rayleigh-Bernard instability associated with the layering. The time constant was circa 15 min per cycle, but this was irregular, with three to five cycles occurring in a 60 min period. Contamination remains a major problem, with excess heat devastatingly quenched; by decreasing electrical resistance of the solution,[2-4] the effects on the cathode can be minimized. Contaminants appear from both electrode and container degradation and leeching, from atmospheric contamination and after temperature cycling. These all inexorably, and unintentionally, add to the electrolytic solution, decreasing the level of deuteron loading, the rate of loading and the maximum heat-producing activity. The heavy water is hygroscopic, therefore kept physically isolated from the air by seals, including several layers of Parafilm M (American National Can, Menasha, WI) and paraffin. All leads near the solution were covered with electrically insulating tubes (medical grade silicone, Teflon, or proprietary materials) used to electrically isolate wires. We continue to avoid chlorine or chloride because of possible explosions resulting from visible light ignition susceptibility because the activation energy with chlorine is only ~17 μJ.

The loading of the palladium from the heavy water, and driving of the reactions through the two electrodes within the reaction container, was obtained by controlled electric current source, or a Keithley 225 at low input, with ±1% accuracy. Electrical voltage sources included HP/Harrison 6525A for transsample potentials up to 3000 V (~±0.5% accuracy). All connections isolated, when possible, with Keithley electrometers for computer isolation. To allow 4-terminal electrical resistance measurements within the loaded PdD_x cathode, a first Keithley 225 electric current source was used to drive the cell and load the cathode, and then a second Keithley 225 electric current source was used to drive the electrical current portion of the 4-terminal electrical resistivity measurement of the palladium. The data from voltage, current, temperatures at multiple sites of the solution, and outside of the cell, the 4-terminal measurement of the cathode's internal electrical conductivity, additional calibration thermometry and other measurements were sam-

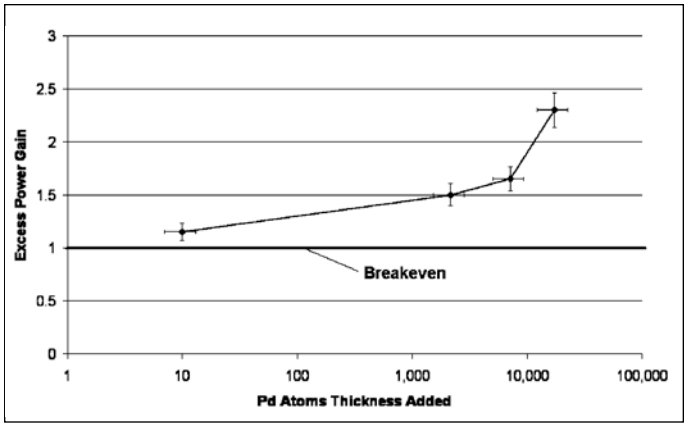

Figure 1. Excess heat correlated with Pd codepositional thickness. Such high impedance metamaterial nanostructured LANR devices have shown power gains more than 200% and short term power gains to ~8000%,[1,2] compared to input energy and to input energy transferred to conventional dissipative devices.

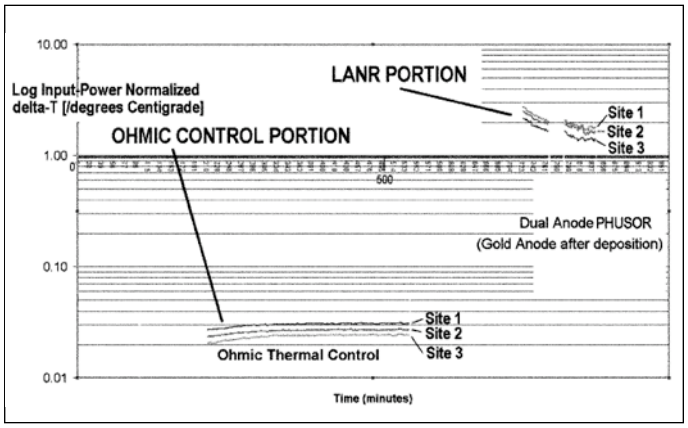

Figure 2. Input power normalized delta-T curves for DAP PHUSOR® LANR. Shows the transient output of one DAP-type (Pd^*/D_2O-$Pd(OD)_2$/Au) LANR device. The graph shows the input power-normalized change.

pled at 0.20 Hz, usually 1 Hz, 22+ bits resolution (Omega OMB-DaqTemp, voltage accuracy 0.015±0.005 V, temperature accuracy <0.6%C) and recorded by computed DAQ. To minimize quantization noise, 1 min moving averages were sometimes made. The noise power of the calorimeter is in the range of ~1-30 mW. The noise power of the Keithley current sources is ~10 nW. Input power is defined as *V I*. There is no thermo-neutral correction in denominator. Therefore, the observed power is a lower limit. The instantaneous power gain [power amplification factor (nondimensional)] is defined as P_{out}/P_{in}, as calibrated by at least one electrical joule control (ohmic resistor) and time integrated for validation. The excess energy, when present, is defined as ($P_{output} - P_{input}$) x time.

The amount of output energy is interfered from the heat released, producing a temperature rise, which is then compared to the input energy. Temperature measurements are made by specialized electrically insulated thermocouples (accuracy ±0.8 K, precision ±0.1 K), RTD and other sensors. Probes were calibrated by Omega IcePoint Cell and core temperatures were maintained by feedback control using a Yellow Spring Thermal Controller Model 72 (bandwidth of 0.2 K) within a Honeywell water circulation zone controlled room (±2.5 K). Thermocouples and other temperature sensors decorated the periphery of the cell, and a multicompartment calorimeter was used. There was an additional heat flow probe at the periphery outside of the core. To minimize contamination, the majority of temperature measurements were outside of the inner core container. Calorimetry is augmented by heat flow measurement, electricity production using thermoelectrics and LANR-driven motors. Outputs are calibrated by ohmic (thermal) controls and dual ohmic (calorimeter) controls, to evaluate and certify possible excess heat. Additional calibration has included adequate Nyquist sampling, time-integration, thermal ohmic controls, waveform reconstruction, noise measurement and other techniques.[2-4] During the experiment, an attempt was made to determine, first, the impact of the direction of the electrical current used for the 4-terminal measurements along the cathode, and second, the impact of the direction of the applied magnetic field intensity obtained from neodymium magnets. The stationary applied magnetic field intensity was circa 0.3 T, and the field was directed either parallel or perpendicular to the applied electric field intensity used to load and drive the LANR device.

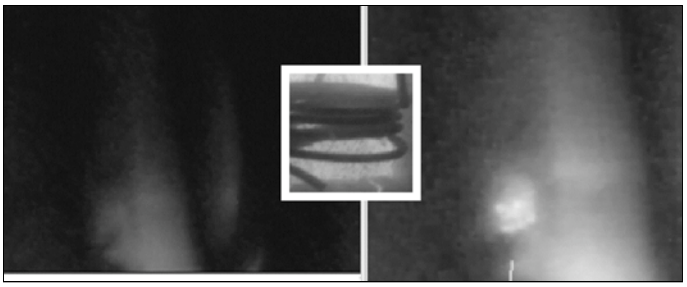

Figure 3. Near-infrared images of DAP LANR cell, before and after activation, with close-up of cathode in visible light (inset).[34]

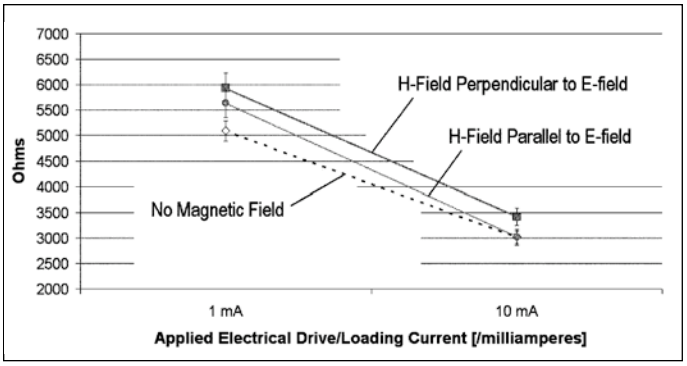

Figure 4. Effect of applied H-field on DAP LANR device's solution electrical resistance.

3. Results: Magnetic Fields

Within the DAP-type ($Pd/D_2O/Au$) LANR device, solution resistances ranged from 800,000 Ω initially to ~5000 Ω. The 4-terminal cathode measurements of electrical resistance of the loaded metal ranged from ~50 to 120 mΩ. For the DAP device, the excess heat was measured as the thickness increased to ~17,000 atoms deep (Figure 1). At that time, the solution was 7.7 mM $Pd(OD)_2$, and the open circuit voltage, V_{oc}, used to determine the effectivity of LANR,[2,3] was 1.46 V. The Pd/D_2O-$Pd(OD)_2$/Au PHUSOR®-type system has an initial cell resistance of circa 868 kΩ, which fell to circa 48.3 kΩ upon final preparation.

For the DAP LANR device, applying a static magnetic field to the LANR system increased the solution's electrical resistance by 10-17%. This is shown in Figure 4. The increase in solution electrical resistance was greatest at lower levels of electrical driving of the LANR system (1 mA vs. 10 mA).

The increase in solution electrical resistance was greatest when the applied magnetic field was perpendicular to the driving electrical field intensity.

Figure 5 shows the time course of the changes to the mag-

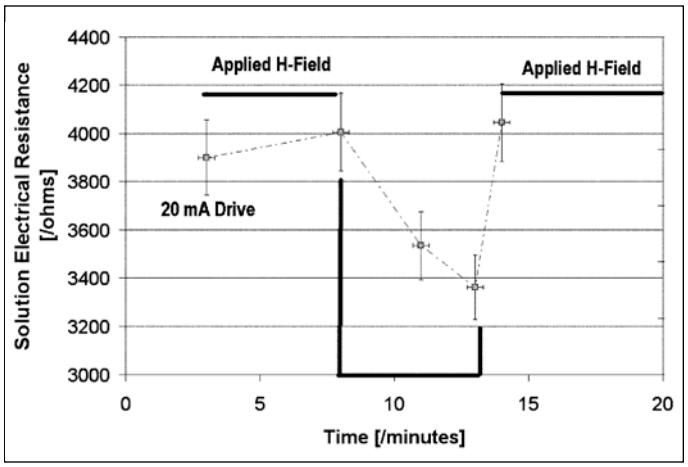

Figure 5. Time course of solution electrical resistance after changes of the applied magnetic field (H-field).

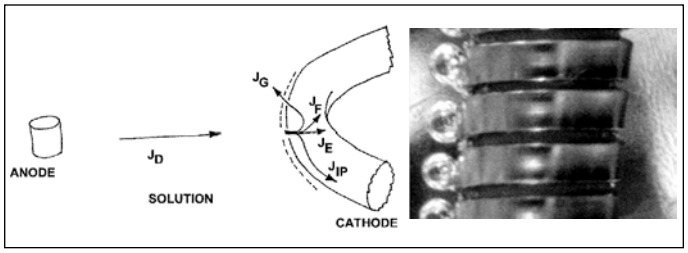

Figure 6. Deuteron fluxes in LANR. Left: Schematic of deuteron fluxes, from solution to loaded metal. Right: Close-up of active LANR cathode.[24]

netic field intensity. The time constant was on the order of minutes.

4. Interpretation: Deuteron Fluxes in LANR

An applied magnetic field in LANR can effect the resistance of the solution and, as will be shown below, that increased resistance can increase metal deuteride loading. Relevant to this analysis were our past studies which examined the impact of laser irradiation on LANR cathodes and reported, in 2003, that it decreases the solution electrical resistance and increases LANR excess heat, but decreases LANR power gain.

Deuteron flux is a key issue in LANR. Nernst calculations of the activities of the electrolyte[51,52] adjacent to a metal electrode have been applied to LANR to derive distributions of deuterium in palladium and the solution. However, because the LANR systems are not at equilibrium, such Nernst calculations are generally not applicable.[53,54] By contrast, unaffected by non-equilibrium, the quasi-1-dimensional (Q1D) model of deuteron loading[53] has been used to analyze deuteron populations and deuteron flow. It has foundation in the known dielectric properties of materials[55] and continuum electromechanics,[56] and has generated the deuteron-flux equations which explain the reason for LANR's difficulty—and the road to success.

Several different deuteron populations and fluxes must be distinguished[57] at the surface of the low hydrogen-overvoltage palladium, with its surface highly populated with atomic, diatomic (D_2) and bulk-entering deuterons.[1,32]

The deuteron fluxes are seen on the left of Figure 6, which is a schematic, simplified representation of the anode, solution and a portion of the cathode along with five types of deuteron fluxes involved in LANR.

The deuteron fluxes are deuteron cationic flow in the solution (J_D), and the four types of deuteron flux in the loaded palladium cathodic lattice (J_E, J_G, J_F and J_{IP}). The latter are the entry of deuterons to the metal lattice ("loading," J_E), movement to gas (D_2) evolution ("bubble formation," J_G), intrapalladial deuteron flux (J_{IP}) flow through the metal (generated by metamaterials), and an extremely tiny loss by the desired fusion reactions (J_F). There is conservation of deuterons with the exception of a loss (J_F) to all putative fusion reactions, which are extremely small, when present.

As Figure 6 shows, cationic deuteron flux (J_D) brings deuterons to the cathode surface to create a cathodic fall and double layer before the electrode surface. It begins far from the cathode surface, in the deuterium oxide (heavy water) located between the electrodes, where the deuterons are tightly bound to oxygen atoms as D_2O. In the absence of significant solution convection, the flux of deuterons (J_D) results from diffusion down concentration gradients and electrophoretic drift by the applied electric field.[53,54,56,58]

$$J_D = -B_D \frac{d[D(z,t)]}{dz} - \mu_D[D(z,t)] \frac{d\Phi}{dz} , \qquad (1)$$

J_D depends on deuteron diffusivity (B_D) and electrophoretic mobility (D) and the applied electric field intensity. At any molecular site across the heavy water solution, the applied electrical energy is a tiny fraction compared to k_BT, so the deuterons migrate by drift ellipsoids of L- and D-deuteron defects in the applied electric field, creating a ferroelectric inscription.[58,59] This D-defect conduction/polarization process augments other charge carriers, ionic drift, space charge polarization and clathrates. The resultant D-defect migration produces a "cathodic fall" of deuterons and an E-field contraction so that most of the voltage drop is at the interface in front of the electrode surface. This concentration polarization may produce very large local electric field intensities, possibly ranging from 10^4 to 10^7 V/cm.[53,54]

From the concentration polarization of deuterons before the cathode, at the inner boundary of the double layer, intermolecular deuteron transfer from the heavy water solution to the metal surface is controlled and limited by electron-limited transfer, which leaves an atomic deuteron on the metal surface. The transfer mechanisms to the palladium surface are driven by infrared vibrations and microwave rotations,[33,59] creating a solution photosensitivity which produces a photo-activated increase of excess energy and loss of power gain.[33]

On the metal surface, the plethora of atomic deuterons either enter the metal ("are loaded") forming a binary alloy,[60-67] or remain on the surface, or form diatomic deuterium gas bubbles (D_2). As a result, palladium has its surface populated with atomic (D) and diatomic deuterium (D_2). Any deuterons which enter the metal are electrically neutralized ("dressed") by a partial electronic cloud, shielding their charge (in a Born-Oppenheimer approximation).[37] The deuterons drift along dislocations and through the lattice and its vacancies, falling from shallow to deeper located binding sites. There is competing obstruction by ordinary hydrogen and other materials at interfaces and grain boundary dislocations. The gas bubbles (D_2) are undesirable producing low dielectric constant layers in front of the electrode, obstructing the electrical circuit. As derived elsewhere,[53] after solving the partial differential equations, and using conservation of mass, and numerically dividing each deuteron flux (J_E, J_G and J_F) by the local deuteron concentration to yield the first-order deuteron flow rates, k_E, k_G and k_F (with units of cm/s, respectively), Equation 2 is the deuteron flux equation of LANR.

$$\kappa_e = \mu_D E - (\kappa_g + \kappa_f) . \qquad (2)$$

Equation 2 is the deuteron loading rate equation. It relates cathodic deuteron gain from the applied electric field to the loss of deuterons from gas evolution and fusion, and teaches many things. The deuteron loading rate equation shows that the deuteron gain of the lattice [through the first order loading flux rate (k_E)] is dependent upon the applied electric field *minus* the flux rate losses of deuterons from gas evolution (k_G) and fusion (k_F). The deuteron loading rate equation, Equation 2, reveals that desired LANR reactions are quenched by electrolysis, which is opposite conventional "wisdom" that LANR is "fusion by electrolysis." Equation 2 also heralds that LANR can be missed by insufficient loading, contamination (effecting k_E, by protons or salt) and by the evolution of D_2 gas, which all inhibit the desired LANR reactions[1,2,53] and leading to the optimal operating point manifolds. This quenching is of prime importance.

Equation 2 can be modified to Equation 3, the modified deuteron loading rate equation, by substituting into it the Einstein relation. There are many important lessons for LANR.

$$k_e = \frac{B_D q V}{L[k_B T]} - (\kappa_g + \kappa_f) . \qquad (3)$$

The first term now has geometric and material factors. B_D is the diffusivity of the deuteron; k_BT is Boltzmann's constant and temperature; q is the electronic charge, and V is the driving applied voltage. Most importantly, dominating the first term is the ratio of two energies (the applied electric energy organizing the deuterons divided by k_BT, thermal disorder). This energy ratio is decisive in controlling the deuteron loading flux in palladium—and thus LANR. Successful LANR experiments reflect the "war" between applied electrical energy which is organizing the deuterons versus their randomization by thermal disorganization.

The second term includes the first-order deuteron loss rates by gas evolution and the desired fusion process(es). The minus sign means that the second term heralds that competitive gas evolving reactions at the metal electrode surface can destroy (quench) the desired reactions. The first-order loading flux rate constant (k_E) is dependent upon the applied electric field intensity minus the first-order gas loss rate constant resulting from gas (D_2) evolution at the cathode (k_G). *This implication is exactly opposite conventional "wisdom" that LANR is "fusion by electrolysis."[1-4] LANR can be missed by insufficient loading, contamination (effecting k_E, by protons or salt) and by the evolution of D_2 gas, which all inhibit ("quench") the desired LANR reactions.[3,4] Note that Equation 3 with the Einstein relation is similar to some flux equations from solid state physics, so there is the question of similarity of deuterons and their holes in Pd to holes and electrons in semiconductor materials.*

5. Interpretation: Impact of H-Field on Loading Rate

We believe the applied magnetic field intensity directly changes the loading rate of deuterons into a metal deuteride. The following explains the reasons, and derives the equations demonstrating the relationship. Consider the role of cathodic photo-irradiation in LANR. In addition to entry into the skindepth layer of the metal, a part of the impact is due to reflection off the cathode back into the double layer. Deuteron injection into the palladium increases (activation energy of ~14 kcal per mol) from microwave rotation and IR vibration for the intermolecular transfer of deuterons to the Pd.[33] Hagelstein, Letts and Cravens[11,12] have also reported both single and dual photon impacts on cathodes as increasing excess heat. As we reported, there is a small and reproducible photo-incremental increase in both the power gain and in the observed excess heat from the coherent irradiation of the cathode, even when heating effects of the beam were included in the calibration. Near the OOP, the optical irradiation increased the excess power from 84.7±10 to 95.5±12 mW. For ~250 mW input electrical power, the irradiation increased the excess power from 79.8±7.6 to 93.3±6.3 mW. Beyond the OOP, the impact of coherent nonionizing radiation upon the cathode is small compared to dark heat production (power gain 1.49±0.005 in the dark, 1.50±0.005 for the laser irradiation, for input power levels which produce 400 mW excess heat). Incremental photo-induced excess power was observed only in the presence of a functioning, active loaded cathode. This photo-induced excess power may be a lower limit. Issues of good optical path geometry, angle of penetration, active irradiated cathodic area, possible double layer interactions, interference with low dielectric constant bubbles formed and skindepth penetration remain relevant and suggest that the actual impact of laser irradiation may be greater.

We discovered that the effects are partially extra-cathodic. Therein lies the "rub." Even though there is an incremental photo-thermoelectric increase in excess heat production changing the net excess power from 1.7 to 1.8±0.1 W, with optical irradiation of the cathode and surrounding solution, there is an additional change. Irradiation of the cathode necessarily results in irradiation of the solution and a photo-induced decrease in the $Pt/D_2O/Pd$ electrical resistance which increased the input electrical power dissipated (not excess). Optical irradiation of the cathodic volume and surrounding solution produces a photo-induced decrease in the effective cell-solution electrical resistance (55-51 kΩ). This increases the input electrical power for the same applied voltage. Because of the relationship between power gain (non-dimensional), excess power and input electrical power (watts), there follows a photo-induced decrease of the power gain, which is noticeable at higher input electrical power levels (2.4-2.3, for 1.3W input).

This paradoxical decrease in the power gain heralds conduction/polarization pathways which lead away from some desired reactions. Exactly why this occurs can be understood by analysis of the modified loading flux equation. Examination of the LANR loading rate equations reveals that there are at least two ways the applied magnetic field can interact in the solution, through the ordering energy ratio and diffusivity of deuterons at the surface (first term), and through the solution resistance (second term).

Assuming a Faradaic efficiency for gas formation of ξ_g per electron, an electric current I, and accounting for the Faraday ratio to the mole, F, then

$$K_g \approx \frac{\xi_g I}{FA[D^+]} \quad . \tag{4}$$

Substituting the electrical admittance with electrical conductivity with geometric factors, yields

$$K_g \approx \frac{\xi_g \sigma_{D_2O} V}{FL[D^+]} \quad . \tag{5}$$

As a result, the modified LANR loading rate equation becomes

$$k_e = \frac{B_D q V}{L k_B T} - \frac{\xi_g \sigma_C V}{FL[D^+]} \quad . \tag{6}$$

The term σ_C/L can be replaced by $1/AR$ (A is the area, R is the solution electrical resistance (ohms). R is in the denominator of the second term. This is a very important equation because, first, the first-order loading rate decreases ("is quenched") with increasing solution electrical conductivity (or decreasing electrical resistance). This equation predicts the response of LANR to an applied magnetic field intensity in an LANR system. If the applied magnetic field intensity is sufficient, this term may dominate, actually increasing the system performance. Increasing the solution electrical resistance (R) increases LANR loading. The converse, through the second term, can end all loading and LANR performance.

Second, in addition, the changes in vectors from the applied magnetic field intensity, with the observed decreased electrophoretic mobility, may be the etiology of some of the morphologies reported by Szpak, Gordon and Mosier-Boss.[19,41,47]

6. Conclusion: Possibility of Increased Loading

An applied magnetic field (~0.3 T) to the high impedance DAP-type LANR system increases the LANR solution's electrical resistance ~10-17%. The time constant for change was on the order of minutes. The incremental resistance increase to an applied H-field is greatest at low input loading and driving electrical currents. The incremental electrical resistance increase to an applied H-field is greatest with the applied H-field perpendicular to the applied driving electrical field (E-field) intensity.

The modified LANR loading rate equation indicates that an applied H-field may increase loading in an LANR system by increasing solution resistance. Our past studies, which examined the impact of laser irradiation on LANR cathodes, has taught us that any change of solution electrical resistance will directly impact LANR performances through the modified deuteron loading rate equation.

In this paper, consistent with that, it is shown that if an applied magnetic field intensity is sufficient, especially perpendicular to the applied electric field intensity and at lower electrical driving currents, an increase in system performance is expected from increased loading, resulting from an increase in solution electrical resistance. In the future, we anticipate reporting and discussing the observed and expected findings in LANR systems, with various arrangements of applied magnetic field intensities.

Acknowledgments

The author thanks Gayle Verner for her meticulous help; Larry Parker Forsley for presenting this lecture; Jeffrey Tolleson, Alan Weinberg, Alex Frank, Charles Entenmann, John Thompson, Peter Hagelstein, Brian Ahern, Pamela Mosier-Boss, Scott Chubb, Jeffrey Driscoll, Richard Kramer, Michael Staker, Jan Marwan, Steven Olasky and Robert Smith for their critique, valued ideas and suggestions; and JET Energy, Inc. and New Energy Foundation for contributing to support this effort. PHUSOR® is a registered trademark of JET Energy, Inc. Images are copyright 2010 JET Energy, Inc. All rights reserved. Protected by U.S. Patents D596,724; D413,659; and other patents pending.

References

1. Swartz, M.R. 2009. "Survey of the Observed Excess Energy and Emissions in Lattice Assisted Nuclear Reactions," *Journal of Scientific Exploration*, 23, 4, 419-436.

2. Swartz, M.R. 2010. "Excess Power Gain Using High Impedance and Codepositional LANR Devices Monitored by Calorimetry, Heat Flow and Paired Stirling Engines," *Proc. Fourteenth International Conference on Condensed Matter Nuclear Science*, D.J. Nagel and M.E. Melich, eds., 123.

3. Swartz, M. and Verner, G. 2006. "Excess Heat from Low Electrical Conductivity Heavy Water Spiral-Wound Pd/D_2O/Pt and Pd/D_2O-$PdCl_2$/Pt Devices," *Condensed Matter Nuclear Science: Proc. 10th International Conference on Cold Fusion*, P.L. Hagelstein and S.R. Chubb, eds., World Scientific Publishing, 29-54.

4. Swartz, M. 1997. "Consistency of the Biphasic Nature of Excess Enthalpy in Solid State Anomalous Phenomena with the Quasi-1-Dimensional Model of Isotope Loading into a Material," *Fusion Technology*, 31, 63-74.

5. Arata, Y. and Zhang, Y.C. 1999. "Anomalous Production of Gaseous ^4He at the Inside of DS-Cathode During D_2-Electrolysis," *Proc. Jpn. Acad. Ser. B*, 75, 281; Arata, Y. and Zhang, Y.C. 1999. "Observation of Anomalous Heat Release and Helium-4 Production from Highly Deuterated Fine Particles," *Jpn. J. Appl. Phys. Part 2*, 38, L774; Arata, Y. and Zhang, Y.C. 2008. "The Establishment of Solid Nuclear Fusion Reactor," *J. High Temp. Soc.*, 34, 2, 85.

6. Celani, F. *et al.* 2010. "Deuteron Electromigration in Thin Pd Wires Coated with Nano-Particles: Evidence for Ultra-Fast Deuterium Loading and Anomalous, Large Thermal Effects," *Proc. Fourteenth International Conference on Condensed Matter Nuclear Science*, D.J. Nagel and M.E. Melich, eds.

7. Dardik, I. *et al.* 2006. "Intensification of Low Energy Nuclear Reactions Using Superwave Excitation," *Condensed Matter Nuclear Science: Proc. 10th International Conference on Cold Fusion*, P.L. Hagelstein and S.R. Chubb, eds., World Scientific Publishing, 61.

8. Dash, J. and Silver, D.S. 2008. "Surface Studies After Loading Metals with Hydrogen and/or Deuterium," *Proc. Thirteenth International Conference on Condensed Matter Nuclear Science*; Dash, J. and Miguet, S. 1996. "Microanalysis of Pd Cathodes After Electrolysis in Aqueous Acids," *Journal of New Energy*, 1, 1, 23.

9. Fleischmann, M. and Pons, S. 1989. "Electrochemically Induced Nuclear Fusion of Deuterium," *J. Electroanal. Chem.*, 261, 301-308, erratum, 263, 187; Fleischmann, M. and Pons, S. 1992. "Some Comments on the Paper 'Analysis of Experiments on Calorimetry of LiOD/D_2O Electrochemical Cells,' R.H. Wilson *et al.*," *J. Electroanal. Chem.*, 332, 1, 33-53; Fleischmann, M. and Pons, S. 1993. "Calorimetry of the Pd-D_2O System: From Simplicity via Complications to Simplicity," *Physics Letters A*, 176, 118-129; Fleischmann, M., Pons, S., Anderson, M., Li, L.J. and Hawkins, M. 1990. "Calorimetry of the Palladium-Deuterium Heavy Water System," *Electroanal. Chem.*, 287, 293.

10. Iwamura, Y., Sakano, M. and Itoh, T. 2002. "Elemental Analysis of Pd Complexes: Effects of D_2 Gas Permeation," *Jpn. J. Appl. Phys. A*, 41, 4642; Iwamura, Y. *et al.* 2005. "Observation of Surface Distribution of Products By X-Ray Fluorescence Spectrometry During D_2 Gas Permeation Through Pd Complexes," in *Proc. 12th International Conference on Condensed Matter Nuclear Science*.

11. Letts, D. and Cravens, D. 2006. "Laser Stimulation of Deuterated Palladium: Past and Present," *Condensed Matter Nuclear Science: Proc. 10th International Conference on Cold Fusion*, P.L. Hagelstein and S.R. Chubb, eds., World Scientific Publishing, 171, 159.

12. Letts, D. and Hagelstein, P.L. 2010. "Stimulation of Optical Phonons in Deuterated Palladium," *Proc. Fourteenth International Conference on Condensed Matter Nuclear Science*, D.J. Nagel and M.E. Melich, eds.; Letts, D., Cravens, D. and Hagelstein, P.L. 2008. "Thermal Changes in Palladium Deuteride Induced by Laser Beat Frequencies," *Low-Energy Nuclear Reactions Sourcebook*, J. Marwan and S. Krivit, eds., Oxford University Press.

13. McKubre, M., Tanzella, F., Hagelstein, P., Mullican, K. and Trevithick, M. 2006. "The Need for Triggering in Cold Fusion Reactions," *Condensed Matter Nuclear Science: Proc. 10th International Conference on Cold Fusion*, P.L. Hagelstein and S.R. Chubb, eds., World Scientific Publishing, 199.

14. Miles, M.H., Hollins, R.A., Bush, B.F., Lagowski, J.J. and Miles, R.E. 1993. "Correlation of Excess Power and Helium Production During D_2O and H_2O Electrolysis Using Palladium Cathodes," *J. Electroanal. Chem.*, 346, 99-117.

15. Miles, M.H. and Bush, B.F. 1994. "Heat and Helium Measurements in Deuterated Palladium," *Transactions of Fusion Technology*, 26, December, 156-159.

16. Miles, M.H. *et al.* 2001. "Calorimetric Analysis of a Heavy Water Electrolysis Experiment Using a Pd-B Alloy Cathode," Naval Research Laboratory Report NRL/MR/6320-01-8526, March 16, 155.

17. Miley, G.H., Narne, G. and Woo, T. 2005. "Use of Combined NAA and SIMS Analyses for Impurity Level Isotope Detection," *J. Radioanal. Nucl. Chem.*, 263, 3, 691-696; Miley, G.H. and Shrestha, J. 2008. "Transmutation Reactions and Associated LENR Effects in Solids," *Low-*

Energy Nuclear Reactions Sourcebook, J. Marwan and S. Krivit, eds., Oxford University Press.
18. Mosier-Boss, P.A. and Szpak, S. 1999. "The Pd/nH System: Transport Processes and Development of Thermal Instabilities," *Il Nuovo Cimento*, 112A, 577-585.
19. Mosier-Boss, P.A., Szpak, S., Gordon, F.E. and Forsley, L.P.G. 2007. "Use of CR-39 in Pd/D Co-Deposition Experiments," *Eur. Phys. J. Appl. Phys.*, 40, 293-303.
20. Mosier-Boss, P.A., Szpak, S., Gordon, F.E. and Forsley, L.P.G. 2009. "Triple Tracks in CR-39 as the Result of Pd-D Co-deposition: Evidence of Energetic Neutrons," *Naturwissenschaften*, 96, 135-142.
21. Pons, S. and Fleischmann, M. 1994. "Heat After Death," *Proc. ICCF4*, EPRI TR104188-V2, 2, 8-1, *Trans. Fusion Technol.*, 26 (4T, Part 2), 87.
22. Srinivasan, M. *et al*. 1992. "Tritium and Excess Heat Generation During Electrolysis of Aqueous Solutions of Alkali Salts with Nickel Cathode," *Frontiers of Cold Fusion: Proc. Third International Conference on Cold Fusion*, H. Ikegami, ed., Universal Academy Press, 123-138.
23. Stringham, R. 2006. "Cavitation and Fusion," *Condensed Matter Nuclear Science: Proc. 10th International Conference on Cold Fusion*, P.L. Hagelstein and S.R. Chubb, eds., World Scientific Publishing.
24. Swartz, M. 2006. "Can a Pd/D_2O/Pt Device be Made Portable to Demonstrate the Optimal Operating Point?" *Condensed Matter Nuclear Science: Proc. 10th International Conference on Cold Fusion*, P.L. Hagelstein and S.R. Chubb, eds., World Scientific Publishing, 29-54.
25. Swartz, M. 1997. "Codeposition of Palladium and Deuterium," *Fusion Technology*, 32, 126-130.
26. Swartz, M. 1997. "Noise Measurement in Cold Fusion Systems," *Journal of New Energy*, 2, 2, 56-61.
27. Swartz, M. 1998. "Patterns of Failure in Cold Fusion Experiments," *Proc. 33rd Intersociety Engineering Conference on Energy Conversion*, IECEC-98-I229, Colorado Springs, CO, August.
28. Swartz, M. 2000. "Patterns of Success in Research Involving Low-Energy Nuclear Reactions," *Infinite Energy*, 7, 31, 46-48.
29. Swartz, M. 2002. "The Impact of HeavyWater (D_2O) on Nickel-Light Water LANR Systems," *Proc. Ninth International Conference on Cold Fusion*, X.Z. Li, ed., 335-342.
30. Swartz, M. and Verner, G. 2005. "Dual Ohmic Controls Improve Understanding of 'Heat after Death,'" *Trans. Amer. Nucl. Society*, 93, 891-892.
31. Swartz, M. and Verner, G. 2004. "Two Sites of Cold Fusion Reactions Viewed by Their Evanescent Tardive Thermal Power," Abstract of ICCF11; Swartz, M. 2005. "Kinetics and Lumped Parameter Model of Excess Tardive Thermal Power," APS Meeting.
32. Swartz, M. and Verner, G. 2010. "Metamaterial Function of Cathodes Producing Hydrogen Energy and Deuteron Flux," *Proc. Fourteenth International Conference on Condensed Matter Nuclear Science*, D.J. Nagel and M.E. Melich, eds., 458.
33. Swartz, M. and Verner, G. 2006. "Photoinduced Excess Heat from Laser-Irradiated Electrically-Polarized Palladium Cathodes in D_2O," *Condensed Matter Nuclear Science: Proc. 10th International Conference on Cold Fusion*, P.L. Hagelstein and S.R. Chubb, eds., World Scientific Publishing, 213-226.
34. Swartz, M., Verner, G. and Weinberg, A. 2010. "Non-Thermal Near-IR Emission Linked with Excess Power Gain in High Impedance and Codeposition Phusor-LANR Devices," *Proc. Fourteenth International Conference on Cold Fusion* , D.J. Nagel and M.E. Melich, eds., 343.
35. Swartz, M. 1998. "Improved Electrolytic Reactor Performance Using pi-Notch System Operation and Gold Anodes," *Transactions of the American Nuclear Association*, Nashville, TN Meeting, 78, 84-85.
36. Swartz, M.R. "Breakeven from LANR PHUSOR Device Systems: Relative Limitations of Thermal Loss in Feedback Loop," *Proc. Fourteenth International Conference on Cold Fusion* , D.J. Nagel and M.E. Melich, eds.
37. Swartz, M.R. 2010. "Excess Heat and Electrical Characteristics of Type B Anode-Plate High Impedance PHUSOR-type LANR Devices," *Journal of Scientific Exploration*, American Chemical Society meeting, in press.
38. Szpak, S. and Mosier-Boss, P.A. 1996. "On the Behavior of the Cathodically Polarized Pd/D System: A Response to Vigier's Comments," *Phys. Letters A*, 221, 141-143; Szpak, S. *et al*. 1995. "Cyclic Voltammetry of Pd+D Codeposition," *J. Electroanal. Chem.*, 380, 1-6.
39. Szpak, S., Mosier-Boss, P.A. and Smith, J.J. 1994. "Deuterium Uptake During Pd–D Codeposition," *J. Electroanal. Chem.*, 379, 121-127.
40. Szpak, S., Mosier-Boss, P.A. and Gordon, F.E. 2007. "Further Evidence of Nuclear Reactions in the Pd/D Lattice: Emission of Charged Particles," *Naturwissenschaften*, 94, 511-514.
41. Szpak, S., Mosier-Boss, P.A., Young, C. and Gordon, F.E. 2005. "Evidence of Nuclear Reactions in the Pd Lattice," *Naturwissenschaften*, 92, 394-397.
42. Szpak, S., Mosier-Boss, P.A., Scharber, S.R. and Smith, J.J. 1992. "Charging of the Pd/nH System: Role of the Interphase," *J. Electroanal. Chem.*, 337, 147-163.
43. Szpak, S., Mosier-Boss, P.A., Miles, M.H. and Fleischmann, M. 2004. "Thermal Behavior of Polarized Pd/D Electrodes Prepared by Co-Deposition," *Thermochim. Acta*, 410, 101-107.
44. Szpak, S., Mosier-Boss, P.A. and Smith, J.J. 1996. "On the Behavior of the Cathodically Polarized Pd/D System: Search for Emanating Radiation," *Phys. Letts. A*, 210, 382-390.
45. Szpak, S., Mosier-Boss, P.A. and Smith, J.J. 1991. "On the Behavior of Pd Deposited in the Presence of Evolving Deuterium," *J. Electroanal. Chem.*, 302, 255-260.
46. Szpak, S., Mosier-Boss, P.A., Boss, R.D. and Smith, J.J. 1998. "On the Behavior of the Pd/D System: Evidence for Tritium Production," *Fusion Technol.*, 33, 38-51.
47. Szpak, S. *et al*. 2005. "The Effect of an External Electric Field on Surface Morphology of Co-deposited Pd/D Films," *J. Electroanal. Chem.*, 580, 284-290.
48. Violante, V., Castagna, E., Sibilia, C., Paoloni, S. and Sarto, F. 2006. "Analysis of Mi-Hydride Thin Film After Surface Plasmons Generation by Laser Technique," *Condensed Matter Nuclear Science: Proc. 10th International Conference on Cold Fusion*, P.L. Hagelstein and S.R. Chubb, eds., World Scientific Publishing, 405, 421.
49. Will, F.G., Cedzynska, K. and Linton, D.C. 1994. "Tritium Generation in Palladium Cathodes with High Deuterium Loading," *Transactions of Fusion Technology*, 26, December, 209-213; Will, F.G. *et al*. 1993. "Reproducible Tritium Generation in Electrochemical Cells Employing Palladium Cathodes with High Deuterium Loading," *J. Electroanal. Chem.*, 360, 161-176.
50. Swartz, M. and Verner, G. 1999. "Bremsstrahlung in Hot and Cold Fusion," *Journal of New Energy*, 3, 4, 90-101.
51. Uhlig, H.H. 1971. *Corrosion and Corrosion Control*, Wiley.
52. Bockris, J. O'M. and Reddy, A.K.N. 1970. *Modern Electrochemistry*, Plenum Press.
53. Swartz, M. 1992. "Quasi-One-Dimensional Model of Electrochemical Loading of Isotopic Fuel into a Metal," *Fusion Technology*, 22, 2, 296-300.
54. Swartz, M. 1994. "Isotopic Fuel Loading Coupled to Reactions at an Electrode," *Fusion Technology*, 26, 4T, 74-77.
55. Von Hippel, A. 1954. *Dielectric Materials and Applications*, MIT Press.
56. Melcher, J.R. 1981. *Continuum Electromechanics*, MIT Press.
57. Swartz, M. 1999. "Generality of Optimal Operating Point Behavior in Low Energy Nuclear Systems," *Journal of New Energy*, 4, 2, 218-228.
58. Swartz. M. 2002. "Dances with Protons: Ferroelectric Inscriptions in Water/Ice Relevant to Cold Fusion and Some Energy Systems," *Infinite Energy*, 8, 44, 64-70.
59. Von Hippel, A., Knoll, D.B. and Westphal, W.B. 1971. "Transfer of Protons through 'Pure' Ice 1h Single Crystals," *J. Chem. Phys.*, 54, 134, 145.
60. Swartz, M.R. 2010. "Optimal Operating Point Manifolds in Active,

Loaded Palladium Linked to Three Distinct Physical Regions," *Proc. Fourteenth International Conference on Condensed Matter Nuclear Science*, D.J. Nagel and M.E. Melich, eds.
61. Hampel, C.A. 1954. *Rare Metal Handbook*, Reinhold Publishing.
62. Hansen, M. and Anderko, K. 1958. *Constitution of Binary Alloys*, McGraw-Hill.
63. Swartz, M. 1994. "Catastrophic Active Medium Hypothesis of Cold Fusion," *Proc. Fourth International Conference on Cold Fusion*, Vol. 4, Sponsored by EPRI and the Office of Naval Research; Swartz, M. 1997. "Hydrogen Redistribution By Catastrophic Desorption in Select Transition Metals," *Journal of New Energy*, 1, 4, 26-33.
64. Papaconstantopoulos, D.A. *et al*. 1977. "Band Structure and Superconductivity of PdD_X and PdH_X," *Phys. Rev.*, 17, 1, 141-150.
65. Wicke, E. and Brodowsky, H. 1978. "Hydrogen in Palladium and Palladium Alloys," *Hydrogen in Metals II*, G. Alefield and J. Volkl, eds., Springer.
66. Teichler, H. 1991. "Theory of Hydrogen Hopping Dynamics Including Hydrogen-lattice Correlations," *J. Less-Common Metals*, 172-174, 548–556.
67. Klein, B.M. and Cohen, R.E. 1992. "Anharmonicity and the Inverse Isotope Effect in the Palladium-Hydrogen System," *Phys. Rev. B*, 45, 21, 405.
68. Swartz, M. 1989. US Patent Application 07/339,976.

About the Author

Dr. Mitchell R. Swartz, ScD, MD, studied electrical engineering, physics and materials at the Massachusetts Institute of Technology, and infectious diseases and oncology at Harvard Medical School. He served a surgical internship, and radiation oncology residency and fellowship, at the Massachusetts General Hospital and other hospitals. At MIT, he developed biomaterial MEM devices, as gas and small molecule sensors. He holds many patents in the U.S. and other countries in medicine and biotechnology and energy production and has two patents in cold fusion, with several pending. Dr. Swartz clinically imaged the first sarcoma by positron emission tomography (PET) and contributed to the development of metabolic imaging. He also developed electrophotochemical pathways for treating human tumors and infectious organisms, and used them to successfully inactivate herpes viruses, bacteria and some types of cancers by engineered colligative dyes with antibonding orbitals and nanoampere electrical currents and other types of activation. Dr. Swartz began research on "pure" water and ice at the Laboratory for Insulation Research at MIT in 1968. In 1989, he applied his technologies to LANR (lattice assisted nuclear reactions), which led to some types of codeposition, optimal operating points, HAD control and one of the first two successful open demonstrations of cold fusion at MIT, for five days in 2003. Today, Dr. Swartz conducts active research on metal hydrides searching for unusual dielectrics and poled ferroelectrics, LANR-driven motors and propulsion devices, and electricity production, for useful commercial and medical applications. He is CTO of JET Energy, Inc., and has been the organizer of the LANR/CF Colloquia at MIT for two decades.

*JET Energy, Inc., Wellesley, MA
Email: mica@theworld.com